



**Universiteit
Leiden**
The Netherlands

Water on well-defined platinum surfaces : an ultra high vacuum and electrochemical study

Niet, M.J.T.C. van der

Citation

Niet, M. J. T. C. van der. (2010, October 14). *Water on well-defined platinum surfaces : an ultra high vacuum and electrochemical study*. Retrieved from <https://hdl.handle.net/1887/16035>

Version: Corrected Publisher's Version

License: [Licence agreement concerning inclusion of doctoral thesis in the Institutional Repository of the University of Leiden](#)

Downloaded from: <https://hdl.handle.net/1887/16035>

Note: To cite this publication please use the final published version (if applicable).

Perfer et obdura, dolor hic tibi proderit olim.

Publius Ovidius Naso, Amores
III:11 (43 BC–17 AD)

2

Experimental techniques and set-up

2.1 Ultra high vacuum

2.1.1 Temperature programmed desorption

In temperature programmed desorption (TPD) the sample is heated with a linear temperature ramp. Depending on the desorption energy, adsorbants will desorb at different temperatures. The amount of desorbing molecules is monitored with a mass spectrometer tuned to the mass of the desorbing species. An aperture is often fitted over the mass spectrometer's ionization region in order to detect only molecules desorbing from the front face of the surface. Without this aperture an additional peak is seen when heating is started from molecules desorbing from the filament used to heat the sample. In case of a density sensitive detector the rate of desorption and the amount of desorbing species have a linear relationship. Ideally only the sample is heated and not, for example, the sample holder, in order to avoid desorption from other surfaces. When the surface temperature becomes high enough to break surface bonds, desorption starts. Assuming that the activation energy is independent of coverage the rate constant (k_d) shows Arrhenius behavior:

$$k_d = A \exp(-E_d/RT) \quad (2.1)$$

where A is a pre-exponential factor, and E_d the desorption energy. The rate of desorption is a convolution of the rate constant and the surface coverage. This leads to peak in the a rate of desorption.¹⁰³ Adsorption energies for the different peaks can be obtained using the Polanyi-Wigner equation

$$r_d(\theta) = -\frac{d\theta}{dt} = \nu(\theta)\theta^n e^{-\frac{E_d(\theta)}{RT}} \quad (2.2)$$

where r is the desorption rate, θ the coverage, t the time, $\nu(\theta)$ the pre-exponential factor, n the desorption order, $E_d(\theta)$ the activation energy, R the gas constant, and T the temperature. Usually TPD spectra are taken for different surface coverages.

Analysis of the data may yield E_d , the surface coverage of the adsorbate, and information on the nature and strength of lateral adatom interactions.^{104,105}

The shape of a TPD curve can be changed by the presence of more than one binding site with differing activation energies for desorption and/or by coverage dependent interactions between adsorbates. The presence of other species changes the TPD curve significantly compared to the clean surface.¹⁰³

2.1.2 Low energy electron diffraction

In low energy electron diffraction (LEED) electrons with an energy of 20–1000 eV are elastically back scattered from a surface. These electrons have a de Broglie wavelength within the same order of magnitude as the interatomic spacing of the surface and will, therefore, undergo diffraction if the surface is well ordered. Positive interference only happens if n and m are integers in the two-dimensional reciprocal lattice vector

$$\mathbf{G} = \Delta \mathbf{k}_{\parallel} = n \frac{2\pi}{a} + m \frac{2\pi}{b}, \quad (2.3)$$

where \mathbf{k}_{\parallel} is the momentum parallel to the surface and a and b are the lattice spacings in two directions. The diffracted beams are collected on a phosphor screen, which will light up by the incident electron beam.¹⁰³

On a stepped surface the electron beam is split into doublets. The direction of the multiplet is perpendicular to the steps.¹⁰⁶ The intensity of the scattered electron beam, I , at angle φ is given by

$$I(\varphi) = c \frac{\sin^2[\frac{1}{2}ka(N+1)\sin\varphi]}{\sin^2[\frac{1}{2}ka\sin\varphi]} \times \sum_{i=-\infty}^{+\infty} \delta[\frac{1}{2}k(N \times a + g)\sin\varphi + \frac{1}{2}kd(1 + \cos\varphi) - i\pi] \quad (2.4)$$

where $N + 1$ is the number of atom rows on a terrace, a the separation of atom rows, g the horizontal shift of the top layer of one step compared to the next step, d the step height, $k = 2\pi/\lambda$ and λ the wavelength. The first term in (2.4) gives the intensity distribution of for a grating with $N + 1$ slits. The second term is sum of δ -functions in the limit of an infinite number of steps, which depend on step width and step height only. The separation between two different delta functions is given by¹⁰⁷

$$\Delta\varphi = \frac{\lambda}{(Na + g)\cos\varphi - d\sin\varphi}. \quad (2.5)$$

The step height can be determined from the relative intensities of the spots at different wavelengths. The spot row to spot splitting ratio is a direct measure of the terrace length. Typical ratios for fcc crystals are given in ref.¹⁰⁸

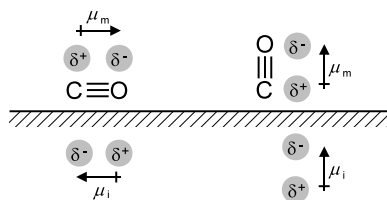


Figure 2.1 Schematic illustration of the surface selection rules for RAIRS with the molecular (μ_m) and image (μ_i) dipoles for a CO molecule lying flat on the surface, and when standing upright.

2.1.3 Reflection absorption infrared spectroscopy

Infrared (IR) spectroscopy is a very popular technique for identifying adsorbates on a metal surface, because of its non-invasive nature. Infrared photons with an energy corresponding to the energy difference between two vibrational levels get absorbed, leaving the molecule vibrationally (or librational) excited. The absorption of photons results in less light of that particular wavelength reaching the detector. A selection rule of IR spectroscopy is that the dipole moment must change during the vibration. In contact with metal surfaces, adsorbed molecules have an image dipole (μ_i) (see figure 2.1). If a molecule is oriented parallel to the surface, the molecular and image dipoles cancel each other. Therefore, even heteronuclear vibrational modes with a dipole parallel to the surface are invisible for IR.

In reflection absorption infrared spectroscopy (RAIRS) use is made of the reflective nature of the metal surface; the surface is used as one of the mirrors in the IR beam path. The light comes in at a grazing angle, in order to make the path through the adsorbate layer as long as possible. Modern IR-spectrometers all use Fourier transform techniques of spectral detection and analysis. The deconvolution of a composite signal allows for simultaneous measurement of all frequencies, significantly reducing the time needed to record an IR spectrum.^{109,110}

2.1.4 Apparatus

POTVIS

All UHV experiments on the Pt(533) crystal have been performed in the apparatus named "POTVIS" ("POT Voor Infrarood Spectroscopie"). It has been described in detail elsewhere,^{111,112} and will only be described briefly here. The main chamber consists of a 1 meter tube with a diameter of ~ 25 cm, which is horizontally mounted on a frame. It is pumped by a turbo molecular pump (Balzers, TPU 450 H, $450 \text{ L s}^{-1} (\text{N}_2)$) below the tube, which is backed by a small turbo molecular pump (Pfeiffer, TMU 071P, $59 \text{ L s}^{-1} (\text{N}_2)$), which in turn is backed by a rotary vane pump (Ilmvac, 302313-09). If necessary a titanium sublimation pump (Balzers, UPK

130A) can be used to lower the pressure further. The system has a base pressure of 2×10^{-10} mbar during experiments.

The sample is located at a copper block at the end of a manipulator, which allows for movement over the entire range of the cylindrical vessel, rotation over 360° , and 2.5 cm in the two perpendicular directions. The Pt(533) sample (Surface Preparation Laboratory, 10 mm diameter, 2 mm thick, cut within 0.1°) is mounted on a tantalum plate, which is screwed onto the copper block. This plate is electrically isolated from the copper block by four sapphire spacers. The temperature of the sample is measured by a K-type (chromel–alumel) thermocouple, spot welded to the crystal. The sample can be cooled to approximately 89 K by running liquid nitrogen through the copper block. It can be heated radiatively by a filament located inside a tantalum cup at the back of the sample and by electron bombardment.

The apparatus is equipped with two quadrupole mass spectrometers (QMS, Balzers, QMS 420 and QMS 422), LEED (VG Microtech), and Fourier transform infrared spectrometer (FTIR, Biorad, FTS 175). The system also has molecular beam facilities. These were not used for the research described in this thesis and shall, therefore, not be described.

The QMS 420 is located inside the main vacuum and is mainly used for residual gas analysis, though it is possible to take TPD spectra with this QMS. The QMS 422 is located in a differentially pumped shield, which can be moved to within 2 mm of the sample and is usually used for TPD measurements.

The FTIR is located on a frame above POTVIS. A flat mirror reflects the external beam onto a 90° off-axis gold coated parabolic mirror with a focal distance of 7.5 inch. This mirror focusses the IR-beam onto the horizontally oriented sample surface under an angle of roughly 85° . An identical parabolic mirror reflects the light up to a third parabolic mirror, which focusses the light on an external liquid nitrogen cooled mercury cadmium tellurium (MCT) detector. A KRS-5 wire grid polarizer is located in front of the CaF_2 view port, in order to filter out horizontally polarized light and, thus, enhance the signal to noise ratio. The entire beam path is purged with dry nitrogen gas, in order to prevent light loss of IR intensity due to absorption by water and CO_2 from air. The absorbance reported in subsection 8 is defined as $A = -\ln(R/R_0)$, where R and R_0 are the reflected intensities with and without adsorbates on the surface.

Water from a Millipore Milli-Q gradient A10 system (18.2 M Ω cm resistance) was deaerated in a glass container by multiple freeze-pump-thaw cycles and then kept at a total pressure of 1.2 bar He (Linde gas, 5.0). The container was connected to a home-built glass capillary array doser¹¹³ located in the infrared cell of the UHV apparatus. Water is dosed directly on the surface by measuring the pressure rise due to the co-dosed helium.

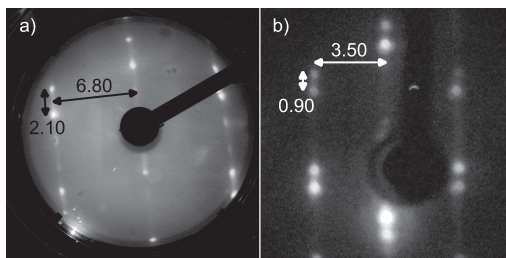


Figure 2.2 LEED images of the clean a) Pt(533) and b) Pt(553) surfaces.

Lion fish

UHV experiments on all other samples have been conducted in the apparatus named "Lion fish". It consists of one chamber, pumped by a turbo molecular pump (Pfeiffer, TMU 521 P, 520 L s^{-1} (N_2)), which is backed by a small turbo molecular pump (Pfeifer, TMH 071 P, 60 L s^{-1} (N_2)), which in turn is backed by a rotary vane pump (Pfeiffer, Duo 10). The system has a base pressure $< 2 \times 10^{-10}$ mbar during experiments.

The sample holder is a copper block located at the end of upright manipulator allowing for 12 cm movement in the up/down direction, 2.5 cm in each perpendicular direction, and 360° rotation. The copper block is electrically isolated from the manipulator by aluminum nitride spacers. The platinum single crystal hangs in a polycrystalline platinum strip. The copper block is liquid nitrogen cooled. The temperature can be varied between 84 and at least 1200 K by radiative heating combined with electron bombardment. The temperature is measured by a K-type thermocouple spot welded to the crystal and controlled with a PID controller (Eurotherm 2416). Absolute temperatures were calibrated by comparing the leading edges of water multilayer desorption to those measured on POTVIS.

The apparatus is equipped with a QMS (Pfeiffer, QME 200) used for both residual gas analysis and TPD spectra and a rear-view LEED/Auger (LK Technologies, RVL 2000/8/R). Water from a Millipore Milli-Q gradient A10 system ($18.2 \text{ M}\Omega \text{ cm}$ resistance) was deaerated in a glass container by multiple freeze-pump-thaw cycles and then kept at a total pressure of 2.0 bar He (Linde gas, 5.0). A warm water bath underneath the container ensures that the H_2O vapor pressure remains constant. The container is connected to a home-built glass capillary array doser which can be moved up to ~ 1.5 cm from the sample.

2.1.5 General procedures

Crystals were cleaned by repeated cycles of Ar^+ (Messer, 5.0) bombardment (POTVIS: $3\text{--}4 \mu\text{A}$, 20 min; Lion fish: $20 \mu\text{A}$, 10 min), annealing between 850 and

1000 K in an oxygen atmosphere (2×10^{-8} mbar), and annealing at 1200 K. Figures 2.2a and b show LEED images taken after cleaning of, respectively, Pt(533) and Pt(553). From these images we deduce a spot row spacing to spot splitting ratio of ~ 3.24 for Pt(533) and ~ 3.9 for Pt(553), which correspond well to the literature values of 3.2787 and 3.8406.^{106–108} The Pt(553) surface was annealed at 1200 K for 3 min in between measurements in order to allow any oxygen induced surface reconstruction to be lifted. This resulted in reproducible TPD spectra.

Water was dosed directly on the surface with $T_s \leq 110$ K at a rate of ~ 0.008 ML s^{-1} by measuring the pressure rise due to the co-dosed helium. Variation of H_2O dosing rates between 0.005 and 0.55 ML s^{-1} have been shown not to influence the morphology of the formed water monolayer on Pt(111).²¹ D_2 (Hoekloos, 2.8) was dosed by background dosing at 2×10^{-7} mbar while cooling down the sample from 500 to 120 K. This produced a full monolayer of D_{ad} . During dosing all filaments were switched off to minimize contamination of H-atoms on the surface. In order to obtain lower coverages the sample was heated with 1 K s^{-1} to a temperature where D desorbs from the surface and cooled down again. Atomic oxygen on the surface was obtained by background dosing of molecular oxygen ($^{16}O_2$ and $^{18}O_2$: Cambridge Isotope Laboratories, 97% isotope purity, $\geq 99.9\%$ chemical purity) at $T_{crys} \approx 100$ K. The surface temperature was then raised with 1 K s^{-1} to 250 K in order to dissociate the molecularly bound oxygen and desorb any remaining molecular oxygen. All reported pressures are uncorrected for ion gauge sensitivity.

For TPD experiments the heating rate was always 1 K s^{-1} . In deuterium co-adsorption experiments $m/e = 2$ (H_2), 3 (HD), 4 (D_2), 18 (H_2O), 19 (HDO), and 20 (D_2O) were monitored with the QMS. We have verified that cracking in the QMS ionizer of HOD and D_2O yields no significant contribution to the signal at $m/e = 18$ at the low signal intensities in experiments for $m/e = 19$ and 20. Therefore, the signal at $m/e = 18$ results only from H_2O within our experimental error. Similarly, the signal at $m/e = 19$ results only from HOD and the signal at $m/e = 20$ only from D_2O . Initially $m/e = 28$ (CO) and 32 (O_2) were measured as well, but no desorption was detected.

In oxygen co-adsorption experiments $m/e = 18$ ($H_2^{16}O$), 20 ($H_2^{18}O$), 32 (O_2), 34 ($^{16}O^{18}O$), and 36 ($^{18}O_2$) were monitored. Preliminary measurements were taken during which also $m/e = 2$ (H_2) and 38 ($H_2^{18}O_2$) were monitored. These measurements showed no desorption of these compounds.

All H_2O coverages are calculated from the integrated TPD peak areas. Our exact definition of a monolayer (ML) is given in chapter 3.3.3. We are not aware of an unambiguous means to determine the integral for 1 ML HOD, D_2O , or $H_2^{18}O$ desorbing from the surface. Therefore, we have used the integral for 1 ML H_2O (desorbing from bare Pt(553)) as a reference in quantifying the amounts of H_2O and HOD. We assume that the cracking ratio in the QMS and channeltron ampli-

fications are similar for these isotopes, because of the relatively small differences in mass/charge ratio. D₂ coverages were calculated assuming a maximum coverage of 1 ML. For O₂ a maximum coverage of 0.25 ML was assumed.

Since H₂O sticks to the stainless steel walls of the chamber, the high vacuum time constant of H₂O leads to an almost stepwise increase in the baseline of our H₂O TPD spectra. A reasonable approximation for the baseline is given by

$$y = y_0 + \frac{1}{2}\Delta y * \left(\tanh \left(\frac{T - T_0}{\Delta T} \right) + 1 \right) \quad (2.6)$$

where Δy is the total increase in the height of the baseline, T_0 is the center of the S-curve, typically slightly before the peak maximum, and ΔT is an arbitrary parameter to smooth out the tanh. Note that the value of ΔT does not affect the total obtained integral, though it may affect the relative intensities of smaller peaks at lower temperatures. We have verified that this baseline correction procedure does not influence the leading edges of our TPD data when fixing ΔT and T_0 for a set of data. All spectra are shown after baseline subtraction.

2.2 Electrochemistry

2.2.1 Electrochemical cell

The electrochemical cells used in this research contain three electrodes (see figure 2.3). Often, a sulphuric or perchloric acid or sodium hydroxide solution is used as the electrolyte, in concentrations ranging from 0.05 to 0.5 M. The electrode of interest is the working electrode. In this case it is a bead type single crystal electrode, hanging in meniscus mode in order to decrease contact of defect sites on the edges of the bead with the electrolyte. A potential difference is applied by a potentiostat (Autolab PGSTAT 30 or PGSTAT 12 or Iviumstat A06075) between the working electrode and a reference electrode. In this thesis a reversible hydrogen electrode (RHE), *i.e.* a platinum wire in a separate compartment where H₂ gas is bubbling through in equilibrium with the electrolyte, is used as reference electrode. The advantage of this electrode is that it automatically corrects for pH effects. A disadvantage is that the bubbling of H₂ makes the potential more noisy, but this can be compensated by putting a 10 μ F capacitor between the reference and a fourth electrode in the main body of the cell. The counter electrode is a platinum flag or wire, which functions as an electron sink or source for the reactions happening at the working electrode. The counter electrode has to be larger than the working electrode, in order for it not to be limiting in the maximum current that can be achieved.

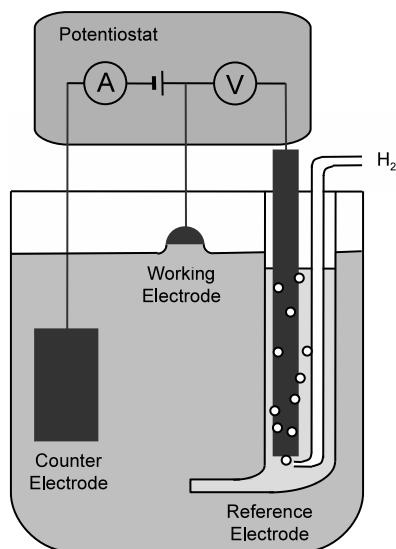


Figure 2.3 A three electrode electrochemical cell with a reversible hydrogen reference electrode.

2.2.2 Cyclic voltammetry

In voltammetric techniques a potentiostat is used to vary the potential linearly while the current response is recorded. The current response is a result of electron transfer to or from the working electrode, which can be related to ad- or desorption processes or to double layer charging. If the potential is swept continuously up and down between two apex potentials, we speak of cyclic voltammetry (CV). It is the most widely used electrochemical technique.¹¹⁴ Typical sweep rates used in the study of single crystal platinum surfaces lie between 1 and 200 mV s⁻¹.

2.2.3 Electrochemical impedance spectroscopy

Impedance is a term used to describe the linear response of a system to a time-dependent signal. Electrical impedance measures the resistance of a system to a sinusoidally alternating current (ac). In electrochemical impedance spectroscopy (EIS) an alternating potential, E_{ac} , is applied on top of a fixed potential E_{dc} :

$$E = E_{dc} + E_{ac} = E_{dc} + E_m \sin(\omega t), \quad (2.7)$$

where E_m is the amplitude of the applied potential and ω the angular frequency. E_m has to be small compared to $E_{m,at,hr,mdc}$. The resulting current density, j , will be out of phase by a phase factor, ϕ :

$$j = j_{dc} + j_{ac} = j_{dc} + j_m \sin(\omega t + \phi), \quad (2.8)$$

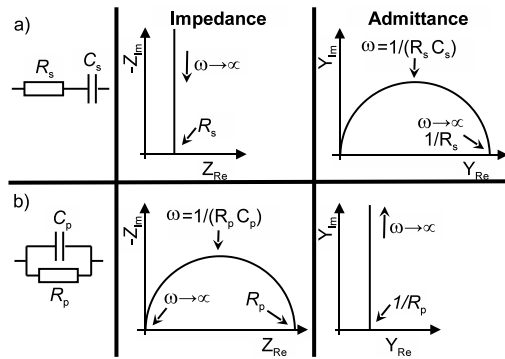


Figure 2.4 Impedance and admittance spectra of RC circuits of a resistance and capacitor in a) parallel and b) series.

where j_m is the amplitude of the resulting current. The electrical impedance, Z , is defined as

$$Z = \frac{E_{ac}}{j_{ac}}, \quad (2.9)$$

which is nothing more than an extension of Ohm's law to cover ac circuits. For a pure resistance, R , $E(t) = j(t)R$ and, therefore, the impedance is independent of the applied frequency:

$$Z_R = \frac{E_m \sin(\omega t)}{j_m \sin(\omega t)} = R. \quad (2.10)$$

The current through a capacitor, C , is the derivative with respect to time of the potential:

$$I_C = C \frac{dE_{ac}}{dt} = CE_m \omega \cos(\omega t) = CE_m \omega \sin\left(\omega t + \frac{\pi}{2}\right). \quad (2.11)$$

Equation 2.11 shows that the current across a capacitor is out of phase with the applied potential by $\pi/2$ or 90° . The impedance of a capacitor, Z_C , using Euler's formula, is now given by

$$Z_C = \frac{E_m e^{i\omega t}}{CE_m i \omega e^{i\omega t}} = \frac{1}{i\omega C} = \frac{-i}{\omega C}, \quad (2.12)$$

where i is the imaginary unit, indicating that the ac voltage at the capacitor is out of phase with the current by -90° .

For combined impedances the total impedance can be calculated using the Kirchhoff laws for combining resistances. For impedances combined, respectively, in series or in parallel the total impedance is given by:

$$Z_s^{\text{tot}} = \sum_n Z_n \quad (2.13)$$

$$\frac{1}{Z_p^{\text{tot}}} = \sum_n \frac{1}{Z_n}. \quad (2.14)$$

The admittance, Y , is defined as $1/Z$. Examples of common RC circuits and the corresponding impedance and admittance spectra, where the imaginary part of the impedance (admittance) is plotted vs. the real part, are shown in figure 2.4. In both circuits R can be derived from the intersection with the real axis, whereas C can be derived from the maximum of the semi circle. Combinations of circuit and spectrum are not unique. If the RC time constants of a circuit are close to one another, semicircles will merge.^{115,116}